# Supplementary Material for Efficiency Droop in Zincblende InGaN/GaN Quantum Wells

D. Dyer,[1] S. A. Church,[1] R. Ahumada-Lazo,[1, 2] M. J. Kappers,[3] M. P. Halsall,[4] P. Parkinson,[1] D. J. Wallis,[3,5] R. A. Oliver,[3] and D. J. Binks[1]

*[1)]Department of Physics and Astronomy & Photon Science Institute, University of Manchester, Manchester M13 9PL, United Kingdom*
*[2)]Tecnologico de Monterrey, School of Engineering and Sciences, Ave. Eugenio Garza Sada 2501, Monterrey, N.L., México, 64849*
*[3)]Department of Materials Science and Metallurgy, University of Cambridge, Cambridge CB3 0FS, United Kingdom*
*[4)]Department of Electrical and Electronic Engineering & Photon Science Institute, University of Manchester, Manchester M13 9PL, United Kingdom*
*[5)]Centre for High frequency Engineering, Cardiff University, Cardiff, CF24 3AA, United Kingdom*

## Calculation of Carrier Density Distribution Amongst QWs.

The Beer-Lambert law is used to calculate the transmitted intensity of light through each layer of the structure in Figure 2d of main article and assuming negligible reflectance at the interfaces between layers, it can be used to determine the fraction of light absorbed in a region of material. The absorption coefficient used in the calculation was obtained from ellipsometry measurements on zb-GaN reported by Baron et al.[1] As mentioned in the main text and illustrated in Figure 2d, it was assumed that the photogenerated carriers diffuse to the nearest QW. Hence, in addition to the carriers directly generated within each QW: the QWs in the middle of the stack (QW # 2-4 in Figure 2d) capture half of the carriers from the barriers to either side; the QW closest to the sample surface will capture all the carriers generated in the top barrier and half from the barrier underneath; and the final QW (QW #5 in Figure 2d) will capture half the carriers photogenerated in the barrier above it and the carriers generated in the InGaN underlayer to a depth varied as shown in Figure 2c. The absorbed power density was converted into carrier density using the carrier lifetime reported previously Church et al. for the 2.5 nm MQW sample[2] and the incident photon energy. Note that the same carrier distribution in wz-InGaN QWs would result in a variation in carrier lifetime for each of the QWs due to the different levels of screening of the electric field, which would have an impact on carrier capture probability. However, lifetime measurements for the zb-SQW sample, shown in Figure S1, indicate that only a small change in the carrier lifetime is observed as the excitation density is significantly increased. Thus, the effect that the variation in carrier lifetime amongst the QWs in the zb-stack was excluded from the calculation.

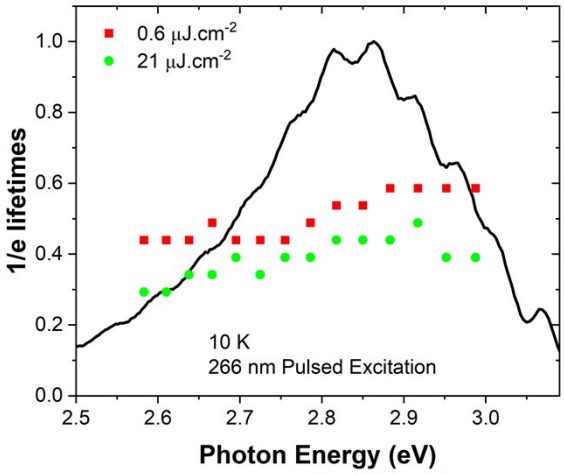


Figure S1. 10 K 1/e decay lifetimes of the zb-SQW sample as a function of emission energy under different excitation densities. The 10 K PL spectrum of the zb-SQW sample excited by a 266 nm pulsed laser is shown in the background for reference.

## Polarised emission.

Figure S2 shows the highly polarised nature of the 10 K photoluminescence (PL) emission from the zb-SQW sample. Although modulated by Fabry-Perot interference fringes, the intensity of the emission along the [1-10] direction is approximately five times the intensity along the [110] direction. Note that the data in Figure S2 was taken with an incident power density of 560 $Wcm^{-2}$, but a high degree of linear polarisation (DOLP) is present for all power densities investigated as shown in Figure S3. The DOLP for the zb-SQW sample can be seen to increase gradually from 0.45 as the power density increases, reaching a maximum value of 0.53. All the zb-QW samples exhibit this trend with increasing power density. However, the 2.5 nm and 7.5 nm zb-MQW samples exhibit a larger DOLP value compared to the zb-SQW and 5 nm zb-MQW samples. Figures S4 – S6 show the power density dependent PL and droop curves resolved along the [1-10] and [110] directions for the zb-MQW samples. The results are similar to the behaviour of the SQW sample shown in Figure 4 of the main article, with the efficiency curves largely independent of the polarisation direction. However, the 2.5 nm MQW sample results show that the droop curves resolved along the two directions overlap less than in the other samples. Thus, for every sample the droop curves are not significantly different from each other and in most cases the droop onsets are the same. The polarisation resolved peak shifts of the emission from the QW layer with incident power density for the sample series are also shown in Figure S7.

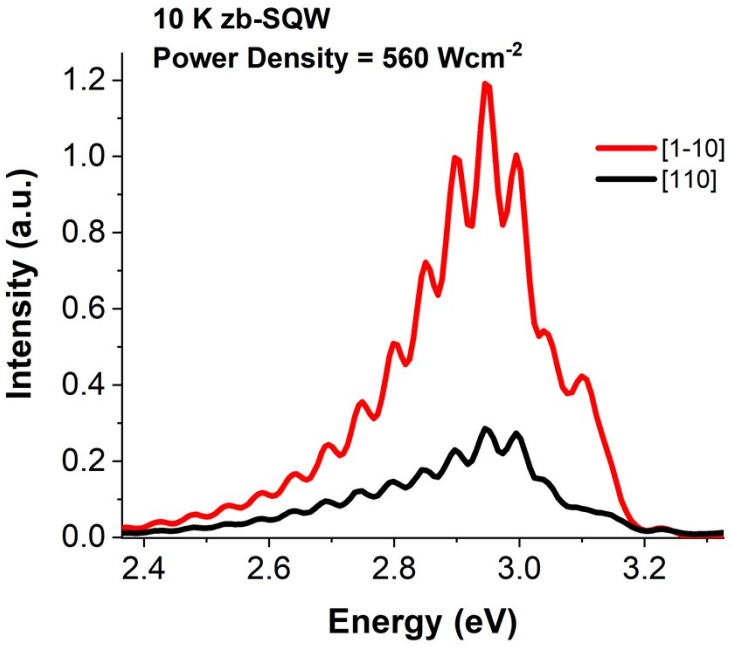


Figure S2. 10 K polarisation resolved PL for the zb-SQW sample along the [1-10] and [110] crystallographic directions. The PL was taken with an incident power density of 560 $Wcm^{-2}$.

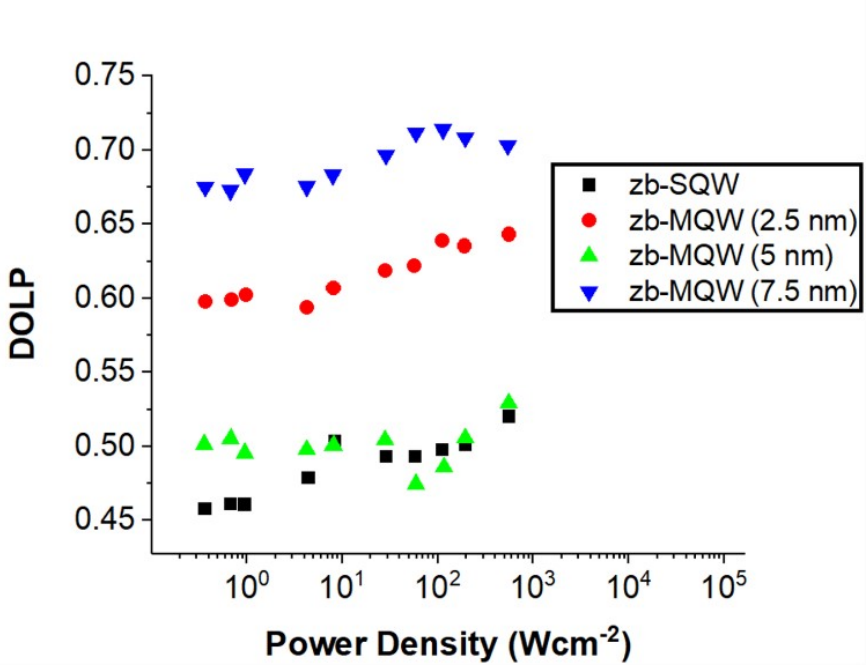


Figure S3. Degree of linear polarisation (DOLP) of the zb-QW samples, taken at 10 K as a function of incident power density.

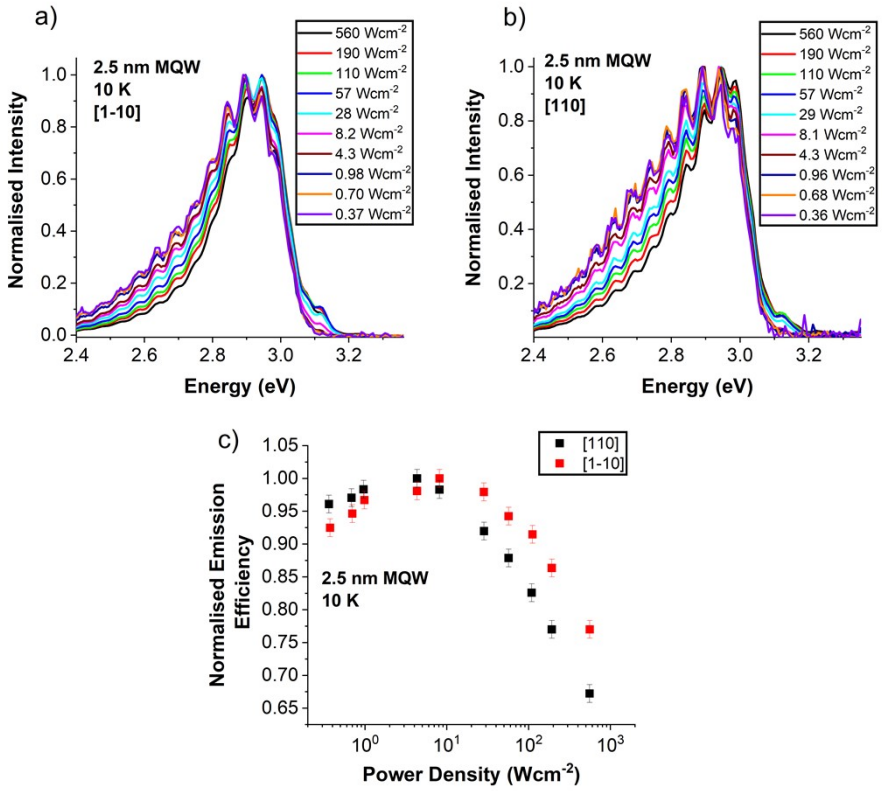


Figure S4. 10 K power density dependent PL for the 2.5 nm MQW sample taken along a) the [1-10] direction and b) [110] direction. c) Efficiency droop curves along these two directions.

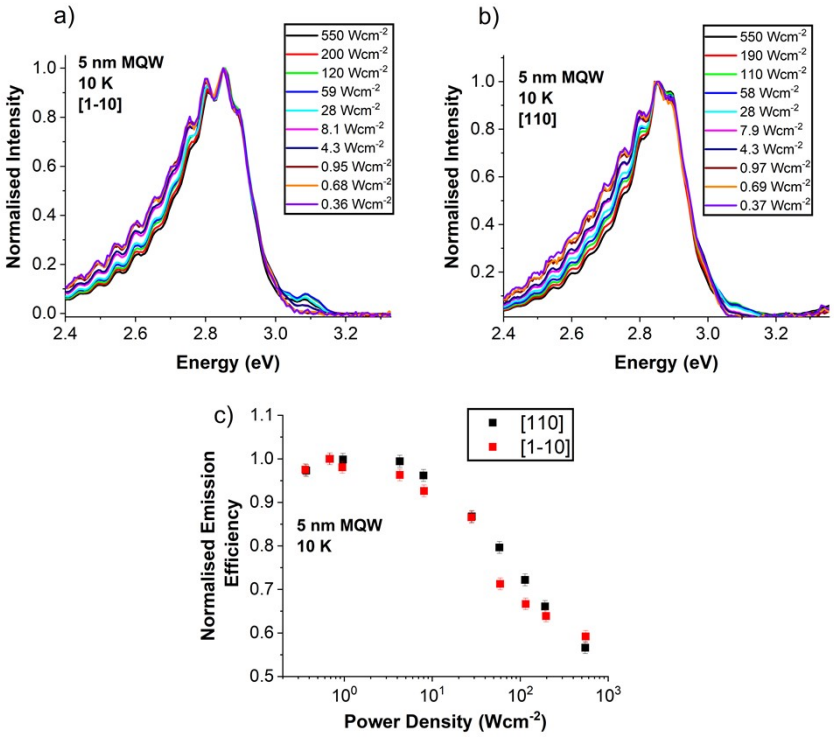


Figure S5. 10 K power density dependent PL for the 5 nm MQW sample taken along a) the [1-10] direction and b) [110] direction. c) Efficiency droop curves along these two directions.

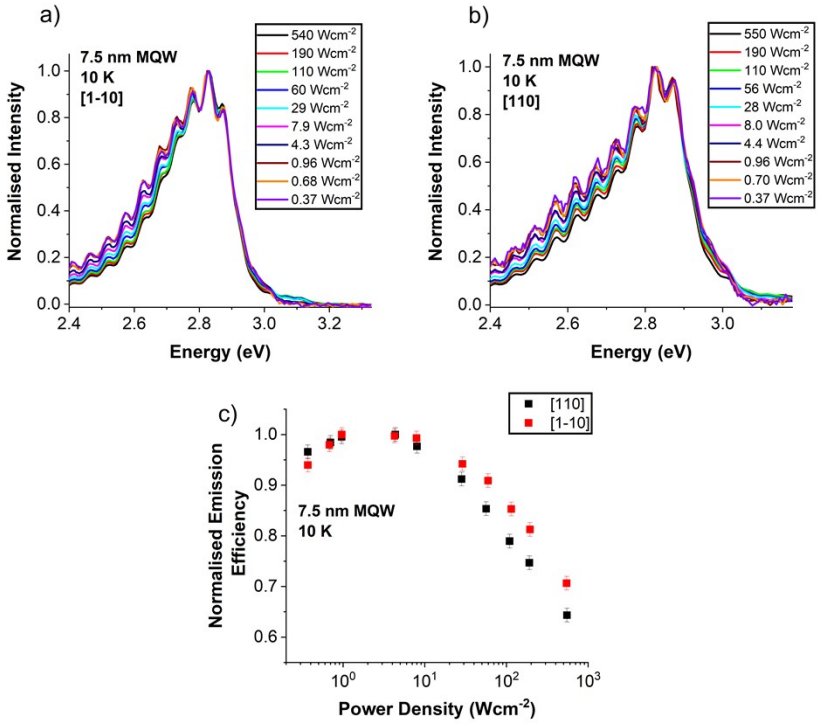


Figure S6. 10 K power density dependent PL for the 7.5 nm MQW sample taken along a) the [1-10] direction and b) [110] direction. c) Efficiency droop curves along these two directions.

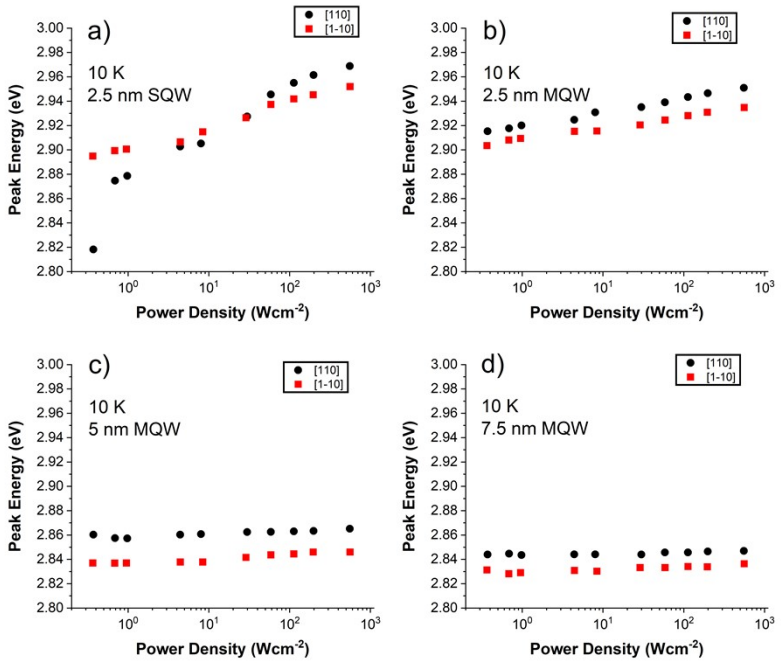


Figure S7. 10 K polarisation resolved peak energy shifts with incident power density for a) SQW, b) 2.5 nm MQW, c) 5 nm MQW and d) 7.5 nm MQW samples.

## Calculation of carrier densities from photoreflection modulation measurements.

As stated in ref 3 since the probe beam is well below the bandgap of zb-GaN, the changes to the refractive index, and thus reflectance, are dominated by the photogenerated carrier density. This is well-described by the Drude model (see equations 7 and 8 in ref 3), which allows the carrier density causing the modulated reflectivity detected by the lock-in amplifier to be determined; the amplitude of the lock-in amplifier signal is converted to reflectance via calibration with a silvered mirror in place of the sample. Repeating this process for a range of incident power densities allows the resulting carrier density generated in the sample to be plotted as a function of incident power density as shown in Figure 5 of the main article.

## References

1 E. Baron, R. Goldhahn, M. Deppe, D. J. As, and M. Feneberg, Influence of the free-electron concentration on the optical properties of zincblende GaN up to 1×1020 cm-3, Physical Review Materials, 2019, **3**, 104603.

2 S. A. Church, M. Quinn, K. Cooley-Greene, B. Ding, A. Gundimeda, M. J. Kappers, M. Frentrup, D. J. Wallis, R. A. Oliver, and D. J. Binks, Photoluminescence efficiency of zincblende InGaN/GaN quantum wells, J. Appl. Phys., 2021, **129**, 175702.

3 M. P. Halsall, I. F. Crowe, J. Mullins, R. A. Oliver, M. J. Kappers, and C. J. Humphreys, Photomodulated Reflectivity Measurement of Free-Carrier Dynamics in InGaN/GaN Quantum Wells, ACS Photonics, 2018, **5**, 4437–4446.